Molecular Catalysis 442 (2017) 107–114

Contents lists available at ScienceDirect

Molecular Catalysis

journal homepage: www.elsevier.com/locate/mcat

Research Paper

Catalytic transfer hydrogenation of ethyl levulinate to γ-valerolactone over a novel porous Zirconium trimetaphosphate

Yongdi Xie[a], Fan Li[b], Jianjia Wang[a], Ruiying Wang[a], Haijun Wang[a,*], Xiang Liu[a], Yongmei Xia[c]

[a] The Key Laboratory of Food Colloids and Biotechnology, Ministry of Education, School of Chemical and Material Engineering, Jiangnan University, Wuxi 214122, China
[b] School of Food Science and Technology, Jiangnan University, Wuxi 214122, China
[c] State Key Laboratory of Food Science & Technology, Jiangnan University, Wuxi 214122, China

ARTICLE INFO

Article history:
Received 18 July 2017
Received in revised form 8 September 2017
Accepted 11 September 2017

Keywords:
γ-Valerolactone
Ethyl levulinate
Catalytic transfer hydrogenation
Zirconium trimetaphosphate
Catalytic mechanism

ABSTRACT

The synthesis of γ-valerolactone (GVL) from catalytic transfer hydrogenation (CTH) of levulinic acid (LA) and its esters is attracting more and more attention due to its wide application in additive, solvent, and precursor. Herein, a novel Zirconium trimetaphosphate (Zr-TMPA) was successfully synthesized and characterized by Fourier transform infrared, N_2 adsorption-desorption, powder X-ray diffraction, scanning electron microscopy, transmission electron microscopy, and NH_3/CO_2-TPD. The as-synthesized Zr-TMPA was used to catalyze the CTH reaction of EL to GVL using isopropanol as the hydrogen donor and solvent. Experimental results shown that Zr-TMPA could catalyze the CTH reaction and 96.2% GVL yield could be achieved at 160 °C for 8 h. Key to this success was attributed to the acid sites and basic sites of the prepared catalyst (Zr-TMPA). Finally, a possible reaction mechanism was proposed.

1. Introduction

At present, the chemical and energy industries rely heavily on the use of fossil resources, which brings a lot of serious problems, so we need to seek an alternative resource for the production of valuable chemicals [1–3]. Biomass, which is a carbon-neutral resource, has been regarded as the renewable resource for the production of valuable chemicals [4,5]. Such as the most common levulinic acid (LA) [6], 5-hydroxymethylfurfural (HMF) [7], 2,5-dimethylfuran [8], furfural [9], furfuryl alcohol [10], γ-valerolactone (GVL) [11], and lactic acid [12], etc. Among them, GVL is one of the most valuable platform molecules, which can be applied directly as a food and fuel additive [13,14]. What's more, it has been used as a precursor for the production of 1,4-pentanediol, 2-methyltetrahydrofuran, perfume, and valeric acid [15–17].

Generally, GVL was mainly prepared from LA and its esters by direct or transfer hydrogenation. The former was usually conducted using various metal catalysis (such as Ru, Ni, Au, Ir, Pt, Pd, Rh) in the presence of external hydrogen [18]. Among them, the Ru- and Ni-based catalysts showed the highest catalytic activity. Tan et al. developed a highly active and stable r-Ru-NH_2-γ-Al_2O_3 catalyst, which obtained 99.1% yield of GVL at 25 °C for 13 h [19]. Jiang et al. found that mixed MgO–Al_2O_3 supported Ni catalysts could achieve 99.7% yield of GVL at 160 °C, 1 h, and 3 MPa H_2 [20]. Although these catalysts have achieved good yield, they are still very difficult to apply in the industry because of the use of precious metals or molecular hydrogen. On the contrary, transfer hydrogenation, which using alcohols or formic acid (FA) as hydrogen donors, has aroused great concern [21]. Ruppert et al. reported the catalytic hydrogenation of LA with FA as a hydrogen source over Ru/C catalysts [22]. But the corrodibility of FA has limited the application in the CTH reaction. In recent years, the use of alcohol as a hydrogen donor has become mainstream in the CTH of LA and its esters to GVL. Most of them are secondary alcohols, for example, Cai et al. reported that 10Cu-5Ni/Al_2O_3 had the highest activity for the CTH reaction of EL to GVL with 2-butanol as the hydrogen donor [23]. Chia and Dumesic found that reduction of LA and its esters to GVL could be achieved using secondary alcohols as the hydrogen donor over ZrO_2 catalysts [24]. It was not difficult to find that the non-precious metals catalysts have caused widespread concern. Recently, many catalysts, such as RANEY® Ni [25], Zr-beta zeolites [26], $Zr(OH)_4$ [27], Ni-Zr [28], Al-Zr [29], Ni-Fe/AC [30], and SnO_2/SBA-15 [31], had been successfully applied to the reduction of LA and its esters to GVL. Especially, song and co-workers continuously reported that

* Corresponding author.
E-mail address: wanghj329@outlook.com (H. Wang).

http://dx.doi.org/10.1016/j.mcat.2017.09.011
2468-8231/

Zr-PhyA, Zr-HBA, and Hf-ATMP were used as efficient catalyst for the CTH of ethyl levulinate (EL) to GVL with isopropanol (IPA) as the hydrogen source and solvent [32–34]. Xue et al. synthesized a porous Zr-CA catalyst that has very high activity for the CTH of LA and its esters to GVL [35]. Although good yield of GVL and conversion of LA and its esters have been achieved, it is still necessary to overcome the low catalyst stability and harsh reaction conditions. Therefore, developing more efficient and stability catalysts for the CTH reaction of LA and its esters to GVL is significant.

Sodium trimetaphosphate (STMP, Schemes 1), which have three phosphate groups in its structure, is mainly used as a starch modifier, dispersant, and stabilizer in the food industry. The strong complexation of phosphoric acid makes it easy to combine with the four-valent metals [36]. In this wook, we synthesized a novel Zirconium trimetaphosphate (Zr-TMPA) catalyst by the reaction of Sodium trimetaphosphate and $ZrOCl_2$ for the CTH reaction of LA and its esters to GVL in the presence of isopropanol. As far as we know, Zr-TMPA as a catalyst for this reduction has not been reported. In addition, the effect of reaction time, temperature, and catalyst dosage for the CTH reaction of EL to GVL were investigated, and a possible reaction mechanism was put forward.

2. Experimental section

2.1. Materials

Sodium hexametaphosphate (SHMPA, AR), γ-valerolactone (98%), Sodium trimetaphosphate (STMPA, 95%), levulinic acid (99%), methyl levulinate (98%), ethyl levulinate (98%), butyl levulinate (98%), $ZrOCl_2{\cdot}8H_2O$ (AR), and ZrO_2 (AR) were purchased from Aladdin Industrial Inc. (Shanghai, China). $SnCl_4{\cdot}5H_2O$ (AR), $TiSO_4$ (AR), pyridine (AR), benzoic acid (AR), ethanol (AR), isopropanol (AR), and naphthalene (AR) were purchased from Sinopharm Chemical Reagent Co. Ltd. (Shanghai, China). Deionized water was produced with a laboratory water-purification system (RO DI Digital plus). All reagents were commercially available and without further purification.

2.2. Catalyst preparation

2.2.1. Synthesis of the Zr-TMPA

In a typical procedure, 10 mmol STMPA and 30 mmol $ZrOCl_2{\cdot}8H_2O$ were dissolved in deionized water (200 mL), respectively. Then, the solution of STMPA was dropwise added to the solution of $ZrOCl_2{\cdot}8H_2O$ in a stirred state. After that, the mixture was continuously stirred for 4 h and then aged for 12 h at room temperature. The white precipitate was separated by centrifugation, thoroughly washed with water and ethanol, and dried at 80 °C under vacuum for 12 h. For comparison, we synthesized three other Zr-TMPA with different Lewis acidity and basicity by the reaction of 10 mmol STMPA and X mmol $ZrOCl_2{\cdot}8H_2O$ (X = 10, 20, 40), which denoted as Zr-TMPA-1, Zr-TMPA-2 and Zr-TMPA-4, respectively. Meanwhile, other catalysts with different metal ions were synthesized using a similar route for Zr-TMPA.

2.2.2. Synthesis of the Zr-HMPA

In a typical procedure, 10 mmol SHMPA and 60 mmol $ZrOCl_2{\cdot}8H_2O$ were dissolved in deionized water (200 mL), respectively. Then, the solution of SHMPA was dropwise added to the solution of $ZrOCl_2{\cdot}8H_2O$ in a stirred state. After that, the mixture was firstly stirred for 4 h and then aged for 12 h at room temperature. The white precipitate was separated by centrifugation, thoroughly washed with water and ethanol, and dried at 80 °C under vacuum for 12 h.

2.3. Catalyst characterization

Fourier transform infrared (FT-IR) spectra were recorded on a Nicolet 360 FT-IR instrument (KBr discs) in the wavenumber range of 4000–500 cm^{-1}. Powder X-ray diffraction (XRD) patterns were obtained on a Bruker D8 Advance diffractometer with Cu-Kα radiation with a scanning rate of 4°/min at 40 kV and 20 mA. Scanning electron microscopy (SEM) images were obtained using a HITACHI S-4800 field-emission scanning electron microscope operated at 15 kV. Transmission electron microscopy (TEM) measurements were performed on a JEOL JEM-2100 microscope operated at 120 kV. The N_2 adsorption-desorption isotherm using a Micromeritics ASAP 2020 provided the porosity properties of catalysts. The X-ray photoelectron spectroscopy (XPS) measurements were implemented on Perkin Elmer PHI 5000 ESCT System. The contents of P and Zr in Zr-HMPA and Zr-TMPA were determined by ICP-AES (Optima 8300). Temperature-programmed desorption of carbon dioxide (CO_2-TPD) was performed on Micromeritics AutoChem II 2920 Chemisorption analyzer. In the experiment, the catalyst was charged into the quartz reactor, and the temperature was increased from room temperature to 300 °C at a rate of 10 °C/min under a flow of He (50 cm^3/min), and then the catalyst was kept at 300 °C for 5 h. After that, the temperature was decreased to 100 °C. CO_2 (50 cm^3/min) was pulsed into the reactor at 100 °C under a flow of He (10 cm^3/min) until the basic sites were saturated with CO_2. The adsorbed CO_2 was removed by a flow of He (50 cm^3/min). When the baseline was stable, the temperature was increased from 60 °C to 600 °C at a rate of 10 °C/min.

Temperature-programmed desorption of ammonia (NH_3-TPD) was performed on Micromeritics AutoChem II 2920 Chemisorption analyzer. The catalyst was charged into the quartz reactor, and the temperature was increased from room temperature to 300 °C at a rate of 10 °C/min under a flow of He (50 cm^3/min), and then the catalyst was kept at 300 °C for 5 h. After that, the temperature was decreased to 100 °C. NH_3/He (10/90, 50 cm^3/min) was pulsed into the reactor at 100 °C under a flow of He (10 cm^3/min) until the acid sites were saturated with NH_3. The adsorbed NH_3 was removed by a flow of He (50 cm^3/min). When the baseline was stable, the temperature was increased from 60 °C to 700 °C at a rate of 10 °C/min.

2.4. Catalytic transfer hydrogenation reaction

In a typical experiment, EL (1 mmol), isopropanol (5 mL) and the catalyst (200 mg) were charged into a stainless reactor of 25 mL equipped with a magnetic stirrer. The reactor was sealed and placed into a preheated oil-bath at a known temperature for the desired time. After the reaction, the liquid samples were analyzed quantitatively by gas chromatography (GC 9790) using naphthalene as the internal standard, and identification of the products was done by GC–MS (ULTRA QP2010). The yield of GVL and the conversion of EL were calculated using the following equations:

$$\text{Yield} = \frac{\textit{Moles of GVL formed}}{\textit{Moles of EL used}} \times 100\%$$

$$\text{Conversion} = \frac{\textit{Moles of EL converted}}{\textit{Moles of EL used}} \times 100\%$$

2.5. Reusability of the Zr-TMPA

To investigate the reusability of the Zr-TMPA catalyst, the catalyst was recovered by centrifugation and washed with ethanol. After drying under vacuum at 80 °C for 18 h, the catalyst was reused for the next run.

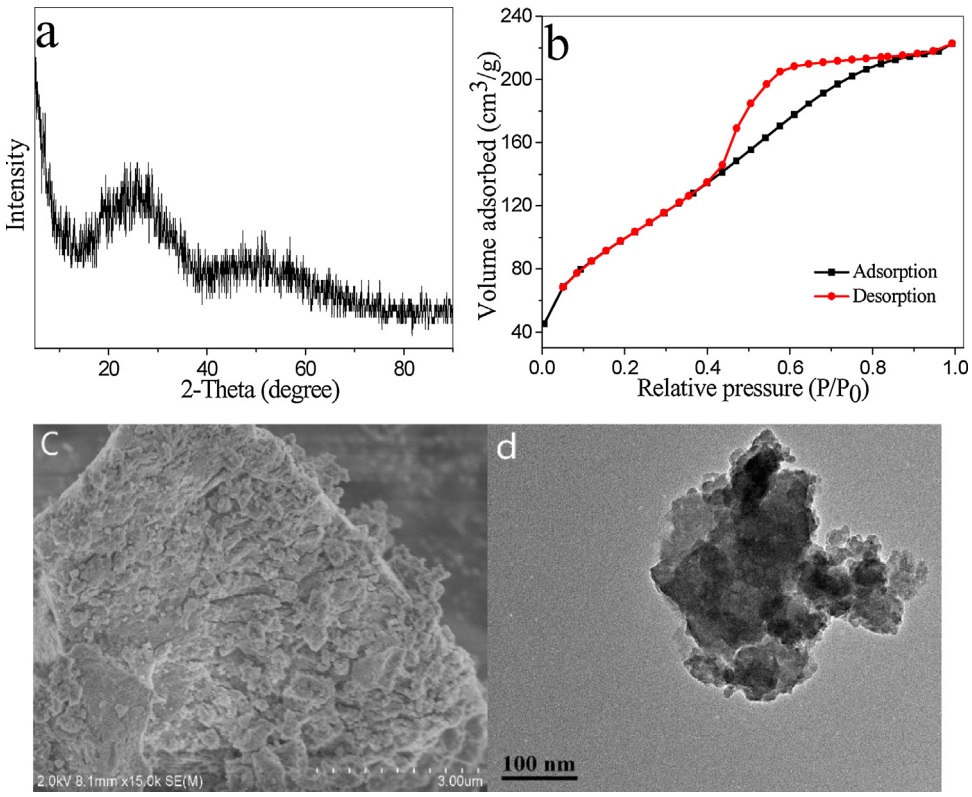

Fig. 1. Characterization of Zr-TMPA. N_2 adsorption-desorption isotherm (a), Powder XRD pattern (b), SEM image (c), and TEM image (d).

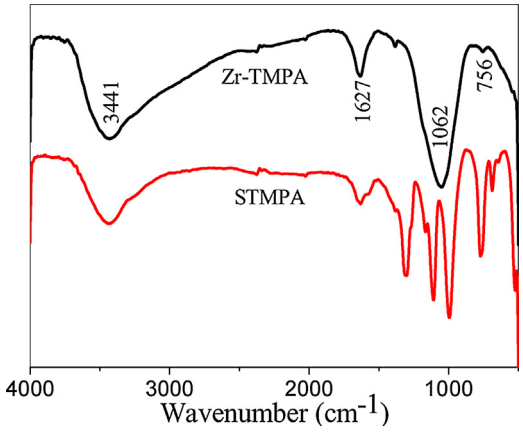

Fig. 2. FT-IR spectra of Zr-TMPA and STMPA.

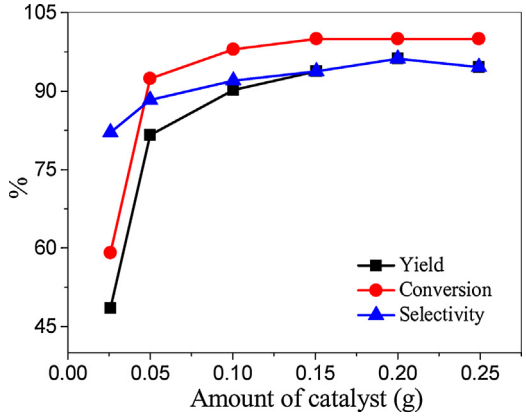

Fig. 3. Effect of catalyst amount. Reaction conditions: 1 mmol EL; 5 mL isopropanol; reaction temperature 160 °C; reaction time 8 h.

3. Results and discussion

3.1. Catalyst characterization

The prepared Zr-TMPA was characterized by N_2 adsorption-desorption isotherm, XRD, SEM, TEM, and FT-IR. The XRD pattern of the Zr-TMPA was shown in Fig. 1a. It was clear that the Zr-TMPA had no X-ray diffraction structure. In general, the presence of weak coordination groups in the catalyst structure resulted in low degree crystallinity. Therefore, the low degree crystallinity of the Zr-TMPA was derived from the only weak coordination groups (phosphate groups) in the structure of the Zr-TMPA. Meanwhile, the XRD pattern had one broad diffraction peak at $2\theta = 26^{\circ}$, suggesting that the Zr-TMPA was amorphous. Simultaneously, SEM and TEM were conducted to examine the surface morphology and internal composition of the prepared catalyst. SEM and TEM images of Zr-TMPA particles are shown in Fig. 1c and d. It can be observed that the Zr-TMPA had no uniform shape and the gaps between the aggregated particles result to the porosity of the catalyst, which results were consistent with the XRD results. In addition, the N_2 adsorption-desorption isotherm of the Zr-TMPA belonged to type IV mode with a hysteresis loop located in the range of 0.4-0.9 relative pressures (Fig. 1b), indicating the presence of irregular mesoporous structure in the Zr-TMPA. The porosity of the Zr-TMPA was caused by the gaps between the aggregated particles. [33] Moreover, the surface area, average pore diameter, and pore volume of Zr-TMPA were 361 $m^2 g^{-1}$, 3.7 nm, and 0.28 $cm^3 g^{-1}$, respectively. All of the above parameters proved that Zr-TMPA, which had low crystallinity and porous structure, could serve as a good catalyst. The FT-IR spectrum of Zr-TMPA and STMPA were shown in Fig. 2. Peaks at 3441 cm^{-1} and 1627 cm^{-1} were attributed to the stretching vibration of hydroxyl groups on the catalyst surface and physically

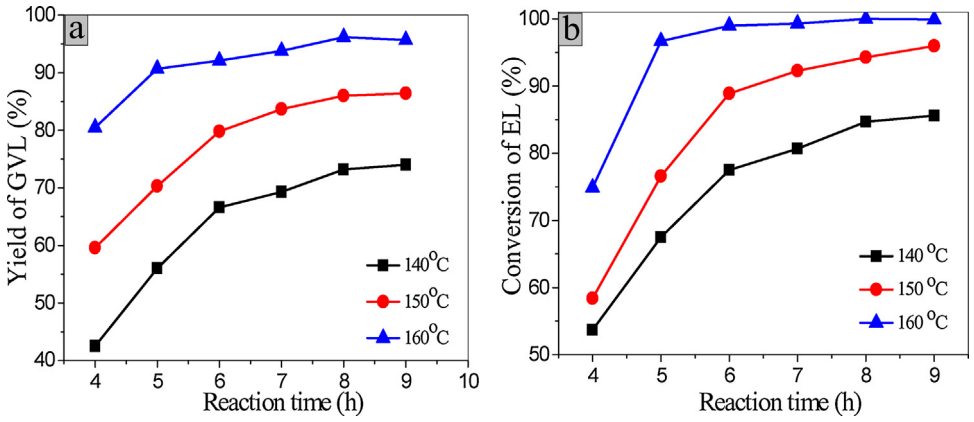

Fig. 4. Effect of reaction time and temperature on the GVL yield (a) and EL conversion (b). Reaction conditions: 0.2 g catalyst; 1 mmol EL; 5 mL isopropanol.

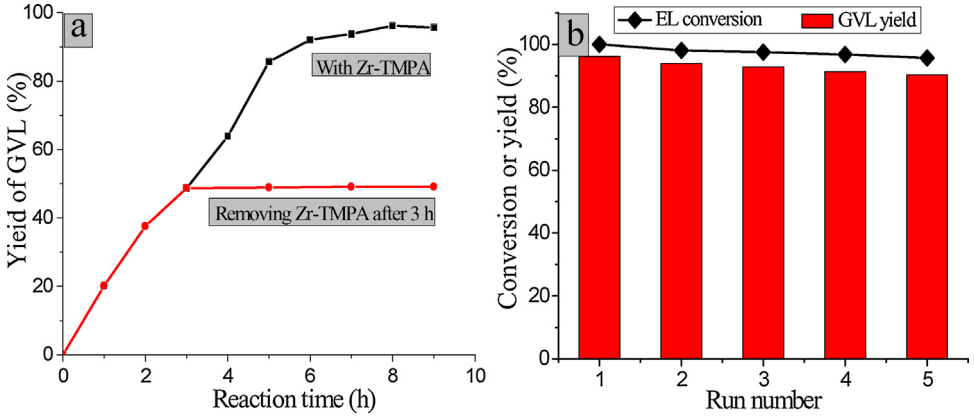

Fig. 5. Leaching experiment of Zr-TMPA for the CTH of EL to GVL (a) and reusability of the Zr-TMPA (b). Reaction conditions: 0.2 g catalyst; 1 mmol EL; 5 mL isopropanol; reaction temperature 160 °C; reaction time 8 h.

adsorbed water. [37] The strong bond at 1062 cm^{-1} was assigned to the stretching vibrations of P–O–Zr network, which could be taken as an evidence of the structural formation of Zr-TMPA. [38] The weak bond at 756 cm^{-1} should be attributed to the P-O-P bending vibration. [39] Thus, it could be deduced that Zr^{4+} was coordinated to phosphate groups. For comparison, other metal (Ti, Sn) –TMPA catalysts and other ligand catalyst Zr-HMPA were also synthesized with similar textural and structural properties (Figs. S1-S4 and Table S1).

3.2. Conversion of EL to GVL over different catalysts

The catalytic research starts from the conversion of EL to GVL with isopropanol as the H-donor and solvent. As shown in Table 1, the CTH reaction did not happen in the absence of catalysts (Table 1, entry 1). When TMPA-based catalysts were used for this reaction, it was obvious that Zr-TMPA showed the highest activity with a full conversion of EL and the GVL yield of 96.2% at 160 °C for 8 h (Table 1, entry 2). In contrary, Ti-TMPA and Sn-TMPA were almost no activity for this reaction, and the byproduct was mainly ispropyl levulinate from transesterification of EL with IPA (Table 1, entry 3–4). Afterward, we used STMPA and SHMPA as a catalyst for the CTH reaction of EL to GVL, only about 1% conversion of EL could be observed (Table 1, entry 5–6). These results indicated Zr was the activity center for the CTH reaction of EL to GVL, and the reaction hardly happens without Zr element. However, Zr-HMPA was also shown the better activity with 99.1% conversion of EL and 94.4% yield of GVL at the same condition (Table 1, entry 7). In contrast, ZrO_2 and $ZrOCl_2$ only obtained a moderate yield of GVL (Table 1, entry 8–9), which revealed Zr-TMPA prepared in this work was an admirable catalyst for the CTH reaction of EL to GVL. The reason for the high activity of the catalyst will be discussed below.

Table 1
Performance of different catalysts for the CTH of EL to GVL.[a]

Entry	Catalyst	Conversion (%)[b]	GVL yield (%)[b]	Selectivity
1	None	0	0	0
2	Zr-TMPA	100	96.2	96.2
3	Ti-TMPA	19.3	0.9	4.7
4	Sn-TMPA	9.0	2.8	31.1
5	STMPA	0.8	0.2	25
6	SHMPA	1.1	0.5	45.5
7	Zr-HMPA	99.1	94.4	95.3
8	ZrO_2	39.4	35.2	89.3
9	$ZrOCl_2$	88.1	45.7	51.9
10[c]	Zr-TMPA	100	95.5	95.5

[a] Reaction conditions: 0.2 g catalyst; 1 mmol EL; 5 mL isopropanol; reaction temperature 160 °C; reaction time 8 h.
[b] Conversion of EL and GVL yield were determined by GC.
[c] The reaction temperature was 170 °C.

3.3. Effect of the amount of catalyst

The effect of the Zr-TMPA dosage on the CTH reaction of EL to GVL was studied at 160 °C with a reaction time of 8 h (Fig. 3). The yield and selectivity of GVL and the conversion of EL increased rapidly when the amount of catalyst increased from 0.025 g to 0.05 g. After the dosage of catalyst was increased to 0.2 g, the yield of GVL and the conversion of EL remained almost unchanged, achieving the maximum yield of GVL (96.2%) and conversion of EL (100%).

Table 2
CTH of LA and its esters into GVL over Zr-TMPA.[a]

Entry	Substrate	Time (h)	Conversion (%)[b]	GVL yield (%)[b]	Selectivity (%)[b]
1	Levulinic acid	4	100	97.7	97.7
2	Methyl levulinate	8	100	96.5	96.5
3	Ethyl levulinate	8	99.9	96.2	96.3
4	Butyl levulinate	8	90.2	83.3	92.4

[a] Reaction conditions: 0.2 g catalyst; 1 mmol EL; 5 mL isopropanol; reaction temperature 160 °C.
[b] Conversion of EL and GVL yield were determined by GC. The other products were mainly isopropyl levulinate obtained by esterification or transesterification.

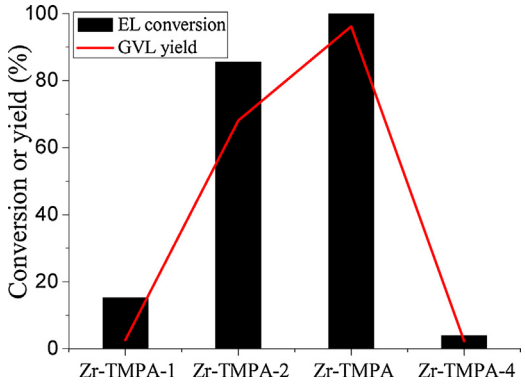

Fig. 6. Effect of catalysts with different Lewis acidity and basicity. Reaction conditions: 0.2 g catalyst; 1 mmol EL; 5 mL isopropanol; reaction temperature 160 °C; reaction time 8 h.

Another 3.8% EL was shown to be converted to isopropyl levulinate that was the leading by-product produced by the transesterification of EL with isopropanol. Hence, 0.2 g of the Zr-TMPA would be the optimum dosage in the subsequent experiments.

3.4. Effect of reaction temperature and time

We studied the effect of reaction time and temperature (Fig. 4). As shown in Fig. 4, it was clear that the reaction time and temperature had a significant effect on the CTH reaction. The yield of GVL and the conversion of EL gradually increased when the temperature increased from 140 °C to 160 °C, which indicated that high temperature was favorable for the CTH reaction of EL to GVL. However, the yield and selectivity of GVL decreased slightly when the reaction proceeded at 170 °C (Table 1, entry 10). This was possibly attributed to by-product generated easily at the higher reaction temperature. Hence, 160 °C was chosen as the best reaction temperature. Similarly, it was found that the yield of GVL and the conversion of EL were relatively low before 5 h due to the formation of isopropyl levulinate. The yield of GVL and the conversion of EL gradually increased by prolonging the reaction time. Finally, 96.2% yield of GVL and 100% conversion of EL could be obtained within 8 h at 160 °C.

3.5. Catalytic effect of Zr-TMPA on different substrates

The CTH reaction of LA and its esters to GVL were further investigated over Zr-TMPA under optimized reaction conditions. As listed in Table 2, LA was easily converted to GVL with 97.7% GVL yield and full LA conversion for only 4 h (Table 2, entry 1). This might be due to the acidity of LA itself that could accelerate the lactonization of 4-hydroxypentanoate. [34] In addition, methyl levulinate could also achieve good results (Table 2, entry 2). However, compared with methyl levulinate and ethyl levulinate, butyl levulinate shown a low activity because of the steric hindrance of butyl (Table 2, entry 4). The above description fully illustrates that Zr-TMPA was an excellent catalyst for the CTH of LA and its esters to GVL.

3.6. The leaching and reusability of the catalyst

The stability and reusability of the catalyst were an important criterion for measuring the quality of a catalyst, hence a leaching experiment was carried out. For compared with the reaction that conducted at 160 °C for 9 h in the presence of Zr-TMPA, another reaction was continued after removing the catalyst at 3 h. As shown in Fig. 5a, the yield of GVL was no further increase after removing Zr-TMPA, suggesting that the active site of Zr-TMPA was not lost and Zr-TMPA was heterogeneous in the reaction. In addition, ICP-AES analysis also shown that Zr leaching was negligible in the solution after the reaction.

To investigate further the reusability of the Zr-TMPA catalyst, recycle tests for the CTH reaction of EL to produce GVL were performed under the optimized reaction condition. EL conversion and GVL yield only slightly decreased after five repeated runs (Fig. 5b). Meanwhile, the reused Zr-TMPA after five cycles was characterized by XRD, FT-IR, SEM, TEM (Fig. S5), N_2 adsorption-desorption, and XPS (Table S2), these results suggested that the structure and properties of the Zr-TMPA were almost unchanged after five cycles. Thence, Zr-TMPA was stable in the reaction system.

3.7. Effect of catalysts with different lewis acidity and basicity

In order to explain the importance of Lewis acidity and basicity to the CTH reaction of EL to GVL, the other three Zr-TMPA with different Lewis acidity and basicity were synthesized and characterized by N_2 adsorption-desorption isotherm, CO_2-TPD and NH_3-TPD (Fig. S6 and Table S3). It shows clearly that there are a big difference between the structural properties and acid/base sites density of the different samples. Although the strength and sun of acid sites decrease with increasing Zr, the base sites density of Zr-TMPA higher than others catalysts, indicating that the content of acid and base sites could be adjusted by varying the molar ratio of SMTPA and zirconium. When the four catalysts were used for the CTH reaction of EL to GVL, it was obvious that the catalytic performance of catalysts followed the order: Zr-TMPA > Zr-TMPA-2 > Zr-TMPA-1 > Zr-TMPA-4 (Fig. 6). These results were consistent with the results of characterization, manifesting that the activity of the catalyst is closely related to the amount of acid and base sites. But the excellent catalytic activity can only be achieved at the optimum acid and base sites ratio.

3.8. Analyze the high activity of the catalyst

As can be seen from the previous analysis that Zr-TMPA showed a high reactivity for the CTH reaction of LA and its esters to produce GVL. Compared with ZrO_2, this high activity may be attributed to their improved surface area and high Lewis acidity and basicity. That being the case, the acidity of ZrO_2 and Zr-TMPA were first analyzed by the XPS and NH_3-TPD (Fig. 7a and b). In general, metal-ions in metal-ligand coordination polymers exhibit Lewis acidity. [40] Hence, the local environment of Zr species in ZrO_2 and Zr-TMPA were inspected by XPS in order to detect the Lewis acidity caused by Zr element. As displayed in Fig. 7a, the binding energies of Zr

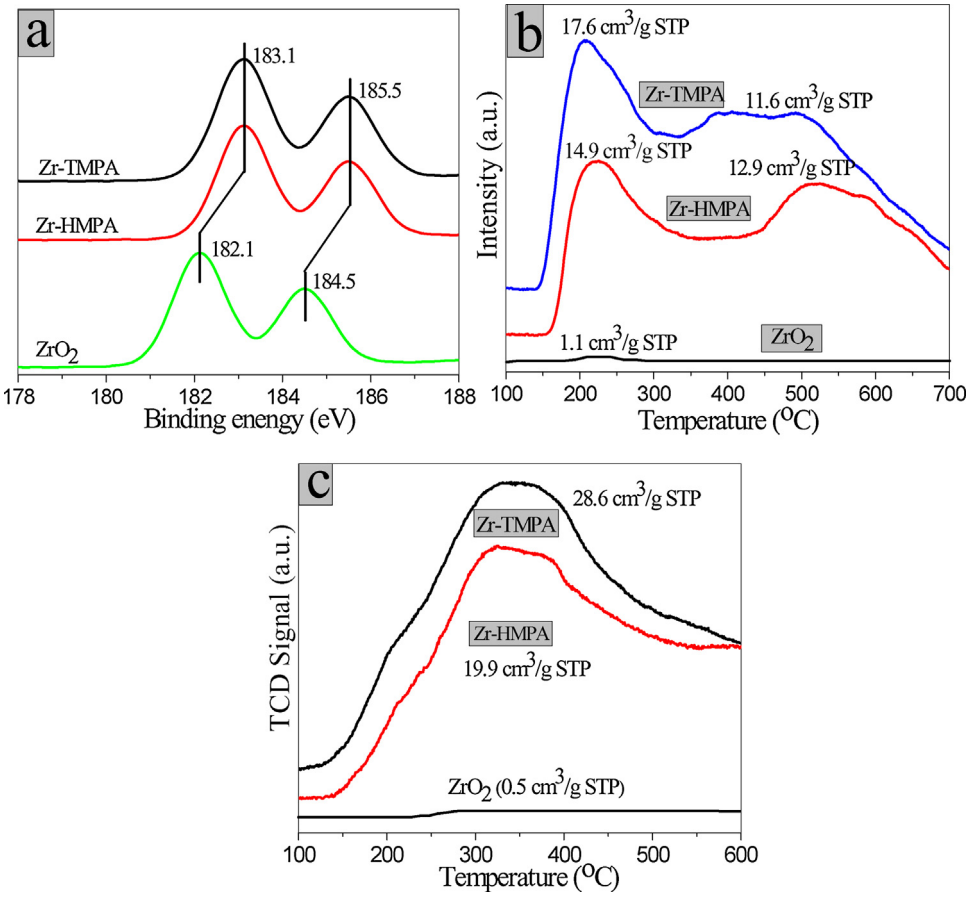

Fig. 7. XPS spectra of Zr 3d (a), NH_3-TPD (b), and CO_2-TPD (c) of Zr-TMPA, Zr-HMPA and ZrO_2.

$3d_{5/2}$ and Zr $3d_{3/2}$ in Zr-TMPA at 183.1 and 185.5 eV were higher than in ZrO_2, manifesting higher positive charge on Zr atoms in the Zr-TMPA, which resulted in stronger Lewis acidity. [41] This was mainly due to the decrease of electron density of Zr caused by the introduction of phosphorus. [32] In addition, the strength and contents of the acid sites of Zr-TMPA and ZrO_2 were determined by NH_3-TPD (Fig. 7b). It can be found that Zr-TMPA have two desorption peaks located at 210 °C and 500 °C, corresponding to the weak and moderate acid strength, and the amounts of acids were 17.6 and 11.6 cm^3/g, respectively. However, ZrO_2 had no appreciable desorption peaks. So it could be inferred that Zr-TMPA had higher acidity than ZrO_2, which was consistent with the results of XPS. The higher Lewis acidity of Zr-TMPA could not only activate carbonyl groups of LA and its esters and also increase the total reaction rate. [32]

It has been reported that the basicity of catalyst was crucial for CTH reaction due to it could increase the dissociation of hydroxyl groups in isopropanol. [33] Therefore, the basicity of Zr-TMPA and ZrO_2 were examined by CO_2-TPD (Fig. 7c) and the amounts of basics were 28.6 cm^3/g and 0.5 cm^3/g, respectively. Song and co-workers had reported that the phosphate groups could increase the basicity of the catalysts. [32,34] Therefore, the high basicity of Zr-TMPA was due to the presence of phosphate groups in its structure. Additionally, Zr-HMPA have similar structures with Zr-TMPA (Scheme S1), which was also used to catalyze LA and its esters to GVL and found that 99.1% conversion of EL and 94.4% yield of GVL were obtained under the optimized reaction conditions. Zr-HMPA was characterized by XRD (Fig. S1), SEM, TEM (Fig. S3), N_2 adsorption-desorption (Fig. S4), XPS (Fig. 7a), and NH_3/CO_2-TPD (Fig. 7b and c). From these characterization results, it was not difficult to find that the structure and property of Zr-HMPA were similar to Zr-TMPA, suggesting that this structure with phosphate groups could significantly increase the basicity of the catalyst.

The acidity and basicity of catalysts we discussed above were very important for the CTH reaction and the structure of the catalysts was also equally important. As shown in Table S1, the surface area, average pore diameter, pore volume of Zr-TMPA were greater than ZrO_2. The more the three parameters was more beneficial to increase the diffusion of reactants to the activity center (Zr) in Zr-TMPA. In summary, the high activity of Zr-TMPA is attributed to the large number of acid-base sites and excellent pore structure.

3.9. Poisoning experiments and reaction mechanism

According to the above discussion and previous studies, [32–35] the acid-base site in the catalyst are critical for the CTH reaction of LA and its esters. From the results of NH_3-TPD and CO_2-TPD, we can clearly see that there are plenty of acid and basic sites on the Zr-TMPA. The basic sites are derived from O^{2-} in the phosphate groups and acid sites originate from the Zr^{4+}. In order to gain more insight toward the role of active sites in Zr-TMPA, Lewis acid and base sites were separately poisoned with pyridine and benzoic acid, respectively. As shown in Table S4, a significant reduce in EL conversion and GVL selectivity was observed when benzoic acid was added (Table S4, entry 2). It is probable that the strong interaction between benzoic acid and base sites. However, the catalytic activity of Zr-TMPA was slightly decreased in the presence of pyridine (Table S4, entry 3). This can be explained by the poor adsorption performance of pyridine on the surface of the catalyst led to the weak poisoning effect. [42] It is concluded that the activity of catalyst is more closely related to the base sites than the acid sites. But the outstanding catalytic effect for the CTH reaction of EL to GVL

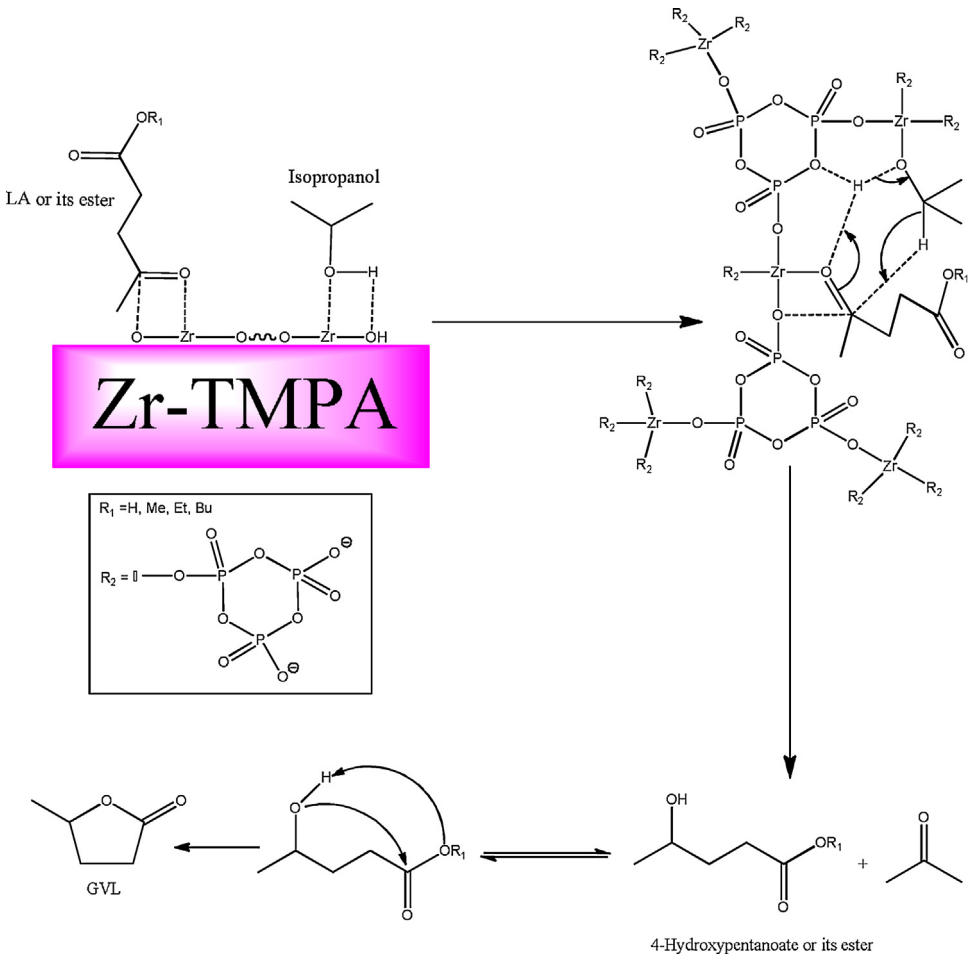

Scheme 1. Possible mechanism for CTH of LA and its esters to produce GVL over Zr-TMPA.

was achieved without adding pyridine and benzoic acid (Table S4, entry 1), which results from the synergistic effect of the Lewis acid and base sites.

Based on this knowledge, a possible reaction mechanism for the CTH of LA and its esters to produce GVL over Zr-TMPA was put forward. As shown in Scheme 1, isopropanol first interacts with the acid-base site (Zr^{4+}-O^{2-}) on Zr-TMPA leading to the separation of isopropanol into the corresponding alkoxide. At the same time, the carbonyl group in LA and its esters can be activated by Zr^{4+}-O^{2-} on Zr-TMPA. Then, hydrogen transfer occurs between the activated carbonyl group and the separated alcohol to form 4-hydroxypentanoate or its esters through a six-member intermediate. Finally, 4-hydroxypentanoate or its esters could be converted to the desired product GVL via intramolecular esterification or transesterification.

4. Conclusion

In summary, we prepared an efficient and robust Zr-TMPA catalyst for the catalytic transfer hydrogenation reaction of LA and its esters to produce GVL. EL conversion of 100% and GVL yield of 96.2% can be obtained under optimized reaction conditions. The Lewis-acidity of Zr and the Lewis-basicity of phosphate groups were responsible for the high reactivity of catalyst. Moreover, repeated tests shown that the Zr-TMPA catalyst could be reused at least five times and its activity is hardly reduced. Finally, a probable reaction mechanism for LA and its esters catalytic transfer hydrogenation was put forward. Hence, this catalyst has great potential for the catalytic conversion of biomass.

Acknowledgment

This work was financially supported by the MOE & SAFEA for the 111 Project (B13025).

Appendix A. Supplementary data

Supplementary data associated with this article can be found, in the online version, at http://dx.doi.org/10.1016/j.mcat.2017.09.011.

References

[1] M.Y. He, Y.H. Sun, B.X. Han, Angew. Chem Int. Ed. 52 (2013) 9620–9633.
[2] M.J. Climent, A. Corma, S. Iborra, Green Chem. 16 (2014) 516–547.
[3] H. Li, Z. Fang, J. Luo, S. Yang, Appl. Catal. B: Environ. 200 (2017) 182–191.
[4] Q. Xu, X.L. Li, T. Pan, C.G. Yu, J. Deng, Q.X. Guo, Y. Fu, Green Chem. 18 (2015) 1287–1294.
[5] L. Wang, H. Wang, F.J. Liu, A.M. Zheng, J. Zhang, Q. Sun, James P. Lewis, L.F. Zhu, X.J. Meng, F.-S. Xiao, ChemSusChem 7 (2014) 402–406.
[6] F.D. Pileidis, M.-M. Titirici, ChemSusChem 9 (2016) 562–582.
[7] R.-J. van Putten, J.C. van der Waal, E. de Jong, C.B. Rasrendra, H.J. Heeres, J.G. de Vries, Chem. Rev. 113 (2013) 1499–1597.
[8] G.-H. Wang, J. Hilgert, F.H. Richter, F. Wang, H.-J. Bongard, B. Spliethoff, C. Weidenthaler, F. Schüth, Nat. Mater. 13 (2014) 293–300.
[9] R. Mariscal, P. Maireles-Torres, M. Ojeda, I. Sadaba, M.L. Granados, Energy Environ. Sci. 9 (2016) 1144–1189.
[10] E. Appiani, R. Ossola, D.E. Latch, P.R. Erickson, K. McNeill, Environ. Sci.: Process. Impacts 19 (2017) 507–516.

[11] X. Tang, X. Zeng, Z. Li, L. Hu, Y. Sun, S. Liu, L. Lin, Renew. Sustain. Energy Rev. 40 (2014) 608–620.
[12] D. Esposito, M. Antonietti, ChemSusChem 6 (2013) 989–992.
[13] I.T. Horváth, H. Mehdi, V. Fábos, L. Boda, L.T. Mika, Green Chem. 10 (2008) 238–242.
[14] Z.H. Zhang, ChemSusChem 9 (2016) 156–171.
[15] D.M. Alonso, S.G. Wettstein, J.A. Dumesic, Green Chem. 15 (2013) 584–595.
[16] M.G. Al-Shaal, A. Dzierbinski, R. Palkovits, Green Chem. 16 (2014) 1358–1364.
[17] L. Xin, Z.Y. Zhang, J. Qi, D.J. Chadderdon, Y. Qiu, K.M. Warsko, W.Z. Li, ChemSusChem 6 (2013) 674–686.
[18] W.R.H. Wright, P. Ralkovits, ChemSusChem 5 (2012) 1657–1667.
[19] J.J. Tan, J.L. Cui, T.S. Deng, X.J. Cui, G.Q. Ding, Y.L. Zhu, Y.W. Li, Catal. Sci. Technol. 6 (2016) 1469–1475.
[20] K. Jiang, D. Sheng, Z.H. Zhang, J. Fu, Z.Y. Hou, X.Y. Lu, Catal. Today 274 (2016) 55–59.
[21] D. Wang, D. Astruc, Chem. Rev. 115 (2015) 6621–6686.
[22] M.R. Agnieszka, J. Marcin, S.-P. Olga, K. Nicolas, S.D. Alexandre, M. Carine, S. Philippe, G. Jacek, Green Chem. 18 (2016) 2014–2028.
[23] B. Cai, X.C. Zhou, Y.C. Miao, J.Y. Luo, H. Pan, Y.B. Huang, ACS Sustain. Chem. Eng. 5 (2017) 1322–1331.
[24] M. Chia, J.A. Dumesic, Chem. Commun. 47 (2011) 12233–12235.
[25] Z. Yang, Y.B. Huang, Q.X. Guo, Y. Fu, Chem. Commun. 49 (2013) 5328–5330.
[26] L. Bui, H. Luo, W.R. Gunther, Y. Román-Leshkov, Angew. Chem Int. Ed. 52 (2013) 8022–8025.
[27] X. Tang, H. Chen, L. Hu, W. Hao, Y. Sun, X. Zeng, L. Lin, S. Liu, Appl. Catal. B: Environ. 147 (2014) 827–834.
[28] H. Li, Z. Fang, S. Yang, ChemPlusChem 81 (2016) 135–142.
[29] J. He, H. Li, Y.M. Lu, Y.X. Liu, Z.B. Wu, D.Y. Hu, S. Yang, Appl. Catal. A Gen. 510 (2016) 11–19.
[30] L. Cai, G.Y. Xu, Y.X. Zhai, X.H. Liu, Y.F. Ma, Y. Zhang, Fuel 203 (2017) 23–31.
[31] S.D. Xu, D.Q. Yu, T. Ye, P.P. Tian, RSC Adv. 7 (2017) 1026–1031.
[32] J.L. Song, B.W. Zhou, H.C. Zhou, L.Q. Wu, Q.L. Meng, Z.M. Liu, B.X. Han, Angew. Chem. Int. Ed. 54 (2015) 9399–9403.
[33] J.L. Song, L.Q. Wu, B.W. Zhou, H.C. Zhou, H.L. Fan, Y.Y. Yang, Q.L. Meng, B.X. Han, Green Chem. 17 (2015) 1626–1632.
[34] C. Xie, J.L. Song, B.W. Zhou, J.Y. Hu, Z.R. Zhang, P. Zhang, Z.W. Jiang, B.X. Han, ACS Sustain. Chem. Eng. 4 (2016) 6231–6236.
[35] Z.M. Xue, J.Y. Jiang, G.F. Li, W.C. Zhao, J.F. Wang, T.C. Mu, Catal. Sci. Technol. 6 (2016) 5374–5379.
[36] M.Y. Gu, D.H. Yu, H.M. Zhang, P. Sun, H. Huang, Catal. Lett. 133 (2009) 214–220.
[37] T.Z. Ren, Z.Y. Yuan, B.L. Su, Chem. Phys. Lett. 374 (2003) 170–175.
[38] Y.J. Jia, Y.J. Zhang, R.W. Wang, J.J. Yi, X. Feng, Q.H. Xu, Ind. Eng. Chem. Res. 51 (2012) 12266–12273.
[39] J. Jiménez-Jiménez, P. Maireles-Torres, P. Olivera-Pastor, E. Rodríguez-Castellón, A. Jiménez-López, D.J. Jones, J. Rozière, Adv. Mater. 10 (1998) 812–815.
[40] H.L. Liu, Y.W. Li, H.F. Jiang, C. Vargas, R. Luque, Chem. Commun. 48 (2012) 8431–8433.
[41] B. Tang, W.L. Dai, X.M. Sun, G.J. Wu, N.J. Guan, M. Hunger, L.D. Li, Green Chem. 17 (2015) 1744–1755.
[42] V.A. Ivanov, J. Bachelier, F. Audry, J.C. Lavalley, J. Mol. Catal. 91 (1994) 45–59.